Iraqi Journal of Biotechnology, 2024, Vol. 23, No. 3, 194-208

Effectivity of Copper Nanoparticle Synthesis by *Fusarium oxysporum* Culture Filtrate as an Antimicrobial Agent against *Streptococcus thoraltensis* and *Proteus mirabilis*

[1]Zahraa A. Saeed Ali , [1]Alaa M. Yaseen AL-Araji

[1] Department of Biology, College of Sciences, University of Baghdad

Received: November 1, 2023 / Accepted: December 20, 2023 / Published: December 30, 2024

Abstract: *Fusarium oxysporum* is a species which is a source of many mycotoxin producers, capable of synthesis Cu nanoparticles as they produce significant amounts of secondary metabolites which act as a reductase and stabilization agent for the produced nanoparticles. The objective of the current study was to demonstrate copper nanoparticles (Cu NPs), biosynthesis was process using *Fusarium oxysporum* culture filtrate has not been previously used in Cu NPs biosynthesis. It was used for the first time as a reducing and stabilizing agent to measure its effectiveness as an antibacterial activity against multidrug-resistant (MDR). Clinical bacterial was isolates, including Gram positive bacteria (*Streptococcus thoraltensis*) and Gram-negative bacteria (*Proteus mirabilis*). *Fusarium oxysporum* isolate were diagnosed by PCR and secondary metabolites determined by GC-MASS. One hundred and sixty specimens of pathogenic bacteria were collected from different sources (wounds, urine, sputum and vagina) then the bacterial isolates were diagnosed as *Streptococcus thoraltensis* and *Proteus mirabilis* by using the Vitek-2 system, biochemical assays, and conventional morphological assessment. *F. oxysporum* culture filtrate done by cultured the fungus using modified Czapek Dox broth media which the cornmeal is added, incubated for 14 days with shaking at 27 ± 2^0C and filtered by Millipore. The biosynthesis of Cu NPs was prepared by adding 1 g of Copper (II) hydrogen carbonate ($CuCo_3$ Cu $(OH)_2$) to 10 ml of *Fusarium oxysporum* culture filtrate, the NPs were diagnosed using modern methods, FT-IR, AFM, FE-SEM, and EDX techniques. The prepared Cu NPs was examined against multidrug-resistant *Streptococcus thoraltensis* and *Proteus mirabilis.* It was concluded that the prepared NPs inhibited pathogenic bacterial isolates. The inhibition for the *Streptococcus thoraltensis* indicated at concentration of 500, 250, 125, and 62.5 mg/ml., and for *Proteus mirabilis* indicated at concentration of 500, 250 and 125 mg/ml.

Keywords: *Fusarium oxysporum*, *Streptococcus thoraltensis*, *Proteus mirabilis*, biosynthesis, antibacterial activity, copper nanoparticles Cu NPs.

Corresponding author: (Email: zahraa.abd1202a@sc.uobaghdad.edu.iq).

Introduction

Fusarium genus, agriculturally significant plant pathogens and opportunistic human infections (1). It contains pathogenic (plant, human, and animal) and non-pathogenic strains, some of which are even capable of bio-controlling certain insects and fungi (2). Numerous studies have demonstrated the remarkable ability of *F. oxysporum* to produce a variety of secondary metabolites with varying activity, including Xanthones, quinones, cyclic peptides, cyclic depsipeptides, alkaloids, jasmonates, anthranilates, cyclic peptides, cyclic depsipeptides,

and terpenoids, with diverse biological activities, including phytotoxicity, antimicrobial activity, cytotoxicity, insecticidal activity, antioxidant activity, and antiangiogenicity. So, *F. oxysporum* is frequently used for manufacture of nanoparticles of different metals that may have uses in biotechnology, pharmaceuticals, industry, and medicine (3). The creation of nanoparticles by biosynthesis is significant because of their lower toxicity in comparison to other biological systems employed for synthesis. Fungi are an excellent biogenic agent due to their wide diversity, straightforward culture methods, superior growth control, effectiveness in terms of both time and money, and ecologically acceptable method of producing nanoparticles. Fungi can produce nanoparticles both intracellularly and extracellularly.

The usage of myco-produced nanoparticles is widespread in a number of industries, including the detection and treatment of disease, the healing of wounds, the preservation of food, the production of textiles, and many more (4). Copper nanoparticles are of incredible interest because of their low price, higher natural abundance, and comparable electrical and thermal conductivity. Their availability and characteristics are comparable to those of other metallic NPs (gold and silver NPs) (5). An important semi-precious mineral, malachite ($Cu_2(OH)_2CO_3$) has recently gained a lot of interest for coatings and catalysts in a variety of applications (6). One of the largest threats to public health today is rising antibiotic resistance in bacterial strains, particularly given the rarity of new and potent antimicrobial drugs being discovered (7). The routine frequent use of antibiotics leads to the widespread and gradual evolution of antibiotic resistance within gram-negative organisms, which is considered one of the most significant problems in the field of medicine (8). Due to the misuse of antibiotics, which causes difficult-to-treat illnesses in humans and animals and higher morbidity and death, antibiotic resistance has become a major problem (9).

In the case of *P. mirabilis*, the antimicrobial resistance is growing and causes the epidemiologic effect of *P. mirabilis* bacteremia (10). *Proteus mirabilis* is the most common of urinary tract infections (11). The *S. thoraltensis* showed high resistance to tetracycline (12). Several strategies have been used to update the antimicrobial chemotherapeutic alternatives that are now reachable (13).

The aim of the study: Evaluation of the efficiency of copper nanoparticle biosynthesis by *Fusarium oxysporum* culture filtrate in inhibiting the growth of pathogenic bacteria *Proteus mirabilis* as a gram-negative and *Streptococcus thoraltensis* as a gram-positive bacterium.

Materials and methods

Isolation and identification of pathogens

Fusarium oxysporum isolate are obtained from the advanced Mycology Laboratory in the Biology Department, Science Collage, University of Baghdad, the isolate activated by culturing fungus on PDA agar prepared by manufacturer`s instructions. It was diagnosed by morphological characteristics according to the colony's morphology, conidiophores and spore shapes, according to Nelson *et al.,* (14) and Watanabe (15), and confirmed the diagnosis by PCR-ITS, Genomic DNA was extracted by DNA kit (ABIOpure, USA) and Purity and concentration of DNA were measured using Nanodrop. The ITS gene is amplified using the

primer pairs ITS1 (TCC GTA GGT GAA CCT GCG G) and ITS4 (TCC TCC GCT TAT TGA TAT GC) (company of Integrated DNA Technologies, USA). A total volume of 25 µl was used for the PCR amplification, which included 1.5µl of DNA, 5 l of Maxime PCR Pre Mix master mix/i-StarTaq (Intron/Korea), 1µl of each primer (10 pmol), and 25µl of distilled water. Thermal cycling was carried out under the following conditions: denaturation at 94 °C for three minutes, then 35 cycles of 94 °C for 45 seconds, 58 °C for one minute, and 72 °C for one minute, with a final incubation at 72 °C for seven minutes. After being stained with red stain, the PCR products were separated by 1.5% agarose gel electrophoresis and then detected by being exposed to ultraviolet light (320nm) (Intron Korea).

Pathogenic bacterial isolates

Total of 160 specimens were employed in this study collected from different ages of patients and different sources (wounds, urine, sputum, vagina). All these bacterial isolates were obtained from clinical specimens, in Medical City of Baghdad during the period from December 2022 to May 2023. The samples were transferred to the University of Baghdad's advanced laboratory and cultured directly using nutrient agar media for 24-48h at $37\pm^{0}$C, after that the bacteria isolates were diagnosed as *Streptococcus thoraltensis* and *Proteus mirabilis* by conventional morphological examination, biochemical tests, and Vitek-2 system.

Preparation of *Fusarium oxysporum* culture filtrate

The crude extracted were extracted by using Czapek Dox Broth media (Himedia) with modification by adding 7 gram of corn flour to 500 ml of broth media. *Fusarium oxysporum* isolate were raised on PDA for three days, and then four blocks (5 mm in diameter) from *F. oxysporum* agar culture were put to the modified Czapek's broth media that had already been prepared (500 ml flasks) and they were incubated for 14 days at $27\pm2C^{o}$ with shaking, After the incubation period, the secondary metabolites were extracted from modified Czapek's media and filtered by Millipore, then GC-MASS applied.

Synthesis of copper nanoparticle (Cu NPs) from *Fusarium oxysporum* culture filtrate

The modified biological synthesis technique was used to create Cu nanoparticles utilizing copper (II) hydrogen carbonate $CuCo_3. Cu(OH)_2$ (Himedia, India) to generate Copper nanoparticles from *F. oxysporum* culture filtrate for the first time. Typical procedure method was done by dissolve (1 g to 10 ml) 5 g of Copper (II) hydrogen carbonate $CuCo_3. Cu(OH)_2$ in 50 mL of *F. oxysporum* culture filtrate. To mix the ingredients, the mixture was dispersed using an ultrasonic bath for 10 minutes and put overnight in a shaker in a dark place (Figure 1).

The leftover fungal culture filtrate was then removed from the solution by centrifuging it at 8000 rpm for 10 minutes and the filtrate was discarded and the sediment was then twice washed with deionized distilled water (D.D.W.) to remove the remaining fungal culture filtrate, and the precipitate was spread in glass Petri dishes. Afterwards dried overnight at 40 °C in the oven to produce a green powder, which was then stored in a dark container for further use (16).

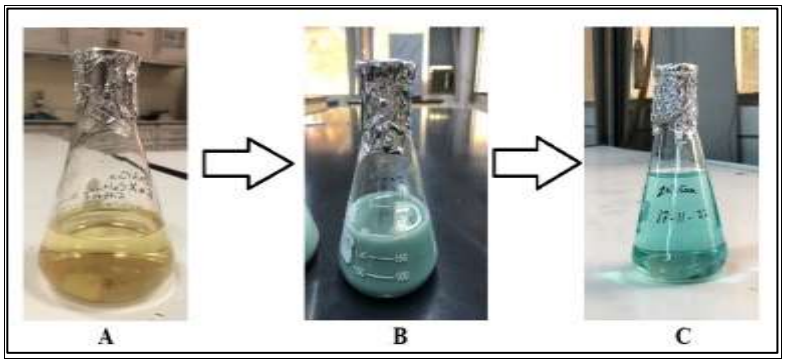

Figure (1): (A) culture filtrate of *Fusarium oxysporum,* (B) the culture filtrate mixed with nano powder, (C) the residual filtrate after nanoparticle separation.

Characterization techniques

FTIR analysis was carried out, which are responsible for metals reduction and for nanoparticle stabilization, the wavelength range utilizing a Fourier transform infrared spectrometer was 4000-400 cm^{-1} (Shimadzu). The AFM identify the morphology and topography of the nanoparticles surface. Nanoparticle samples in a thin film was applied to a glass slide by dropping 100 µl with a five-minute drying time. The slides then became available for analysis and scanned with an AFM AA-3000, USA. EDX analysis was performed on Thermo Scientific Axia ChemiSEM Scanning electron microscopy (SEM) and carried out at an acceleration voltage of 20.0 kV. To ascertain the morphology, size, and shape of copper NPs, FE-SM analysis was carried out, measurements were done by Inspect F 50 FE-SEM scanning electron microscope.

Antibiotics susceptibility test

The Kirby-Bauer approach, which makes use of the disk diffusion technique, bacterial isolates subjected to several antibiotic classes (Piperacillin Aztreonam, Imipenem, Meropenem, Gentamicin, Amikacin, Ciprofloxacin, Levofloxacin, Gentamicin, Ceftazidime and Norfloxacin) for *P. mirabilis*, and (Meropenem, Levofloxacin, Azithromycin, Tetracycline, Chloramphenicol, Vancomycin, Ampicillin, Erythromycin, Ofloxacin and Penicillin) for *S. thoraltensis*. By measuring the diameter of the inhibitory zone, the susceptibility of bacterial isolates to an antibiotic was identified. According to the recommendations of the Clinical Laboratory Standard Institute (CLSI, 2022), reference tables were utilized to categorize the isolates as being either sensitive (S), intermediate (I), or resistant (R) to the antibiotic.

Antibacterial activity of cu nanoparticles

The antibacterial activity of Cu Nanoparticles against the multi-drug resistant *P. mirabilis* and *S. thoraltensis* was directed by preparing standardized inoculum (0.5 McFarland's standard, 1.5x108 CFU/ml), it was poured onto sterile plastic Petri dishes filled with Muller-Hinton agar (MHA) and a cotton swap spreader was used to spread it out, A sterile corkborer was used to create 4 wells, 4 mm diameter in the agar medium. Then prepared the first concentration (stock solution) of Cu NPs by dissolving 1 g of Cu NPs powder in 10 ml of D.D.W. and using vortex to dissolving the powder completely, four series dilutions of Cu NPs were prepared from the first concentration (stock solution). The previously prepared Cu NPs solutions (20 µL) were then poured into the corresponding wells. The loaded plates

were incubated for 24 h at 37 C^0. After incubation, the extent of the produced inhibition zone around the well was measured and determined in mm, demonstrating Cu NPs antibacterial activity.

Statistical analysis

To find the impacts of the various factors on the research parameters, the Statistical Analysis System (SAS) application was employed. In this study, means were compared utilizing the ANOVA approach (analysis of variance) known as the test for the least significant difference (LSD).

Results and discussion

Identification of *Fusarium oxysporum* by PCR

The result of the extraction of *Fusarium oxysporum* DNA showed that the Purity was 1.6 – 1.8 and the concentration of DNA was (290 µg). The *F. oxysporum* isolate's identification was based on the ITS region. *F. oxysporum* isolate were effectively used to amplify the intergenic spacer region. The isolate yielded a unique product size of approximately 550-600 bp as shown in (Figure 2). As demonstrated by other studies on the identification, description, and genetic diversity of the Fusarium strain, which produced amplicons in the 600 pb size range when the rDNA region of the isolates was amplified (17). The Fusarium species specific PCR primers, ITS1 and ITS4 can provide a fast and accurate tool for the Characterization and identification of Fusarium species (Figure 3).

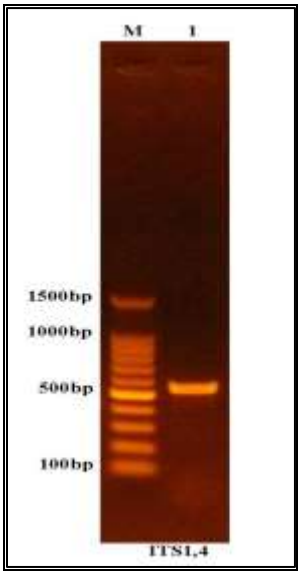

Figure (2): PCR product electrophoresis on an agarose gel with a band size of 550 bp. Product: DNA ladder (100), lane (1) *Fusarium oxysporum*, electrophoresis on 2% L.

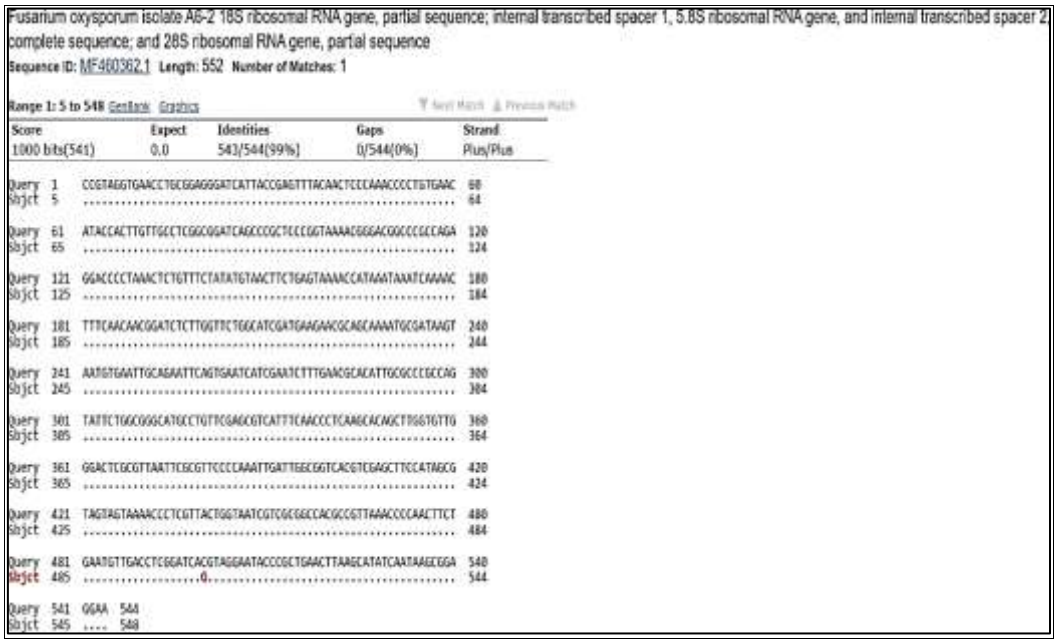

Figure (3): *Fusarium oxysporum* internal transcribed spacer 1, partial sequence, 5.8S ribosomal RNA gene and internal transcribed spacer 2, whole sequence, 28S ribosomal RNA gene, partial sequence was all sequenced. Sequence ID is MF 460362.One length: 552 Matches Found: 1.

Pathogenic bacterial isolation

During the study period of December 2022 to May 2023, a total of 160 clinical specimens were cultured, 24 specimens out of the 160 tested positive for bacteria giving a prevalence rate of 15%. The number of collected specimens consisted of 5 (3.125%) wounds, 10 (6.25%) urine specimens, 8 (5 %) sputum specimens, and 1 (0.625 %) vagina specimen (Table 1). Bacterial isolates 15 (9.375%) *Proteus mirabilis* and 9 (5.625%) *streptococcus* and just one 1 (0.625 %) *Streptococcus thoraltensis* species were diagnosed. This result was consistent with the study of (18).

Table (1): Prevalence of human pathogenic bacteria among clinical specimens.

Source	Number of Samples	Number negative	Number positive	Prevalence positive rate (%)	No. of *P. mirabilis* Isolates	No. of *Streptococcus* Isolates
Wounds	40	35	5	3.125%	4	1
Urine	41	31	10	6.25%	6	4
Sputum	46	38	8	5%	5	3
Vagina	33	32	1	0.625 %	-	1
Total	160	136	24	15%	15	9

Vitek-2 compact system for *S. thoraltensis* and *P. mirabilis*

From 160 isolated specimens, only 15 (9.375 %) were diagnosed as *P. mirabilis* and 1 (0.625 %) were diagnosed as *S. thoraltensis*. The selected bacterial isolates were identified and species confirmed by using Vitek-2 compact system. *P. mirabilis* had 93% Table 2 and *S. thoraltensis* had 91% probability (Table 3). Studies conducted by (19,20) successfully identified Gram-positive and negative bacteria using the VITEK 2 system.

Table (2): Vitek-2 result of *Proteus mirabilis.*

Identification Information	Analysis Time:	5.65 hours	Status:	Final
Selected Organism	93% Probability	*Proteus mirabilis*		
	Bio number:	0013000140440230		

Table (3): Vitek-2 result of *Streptococcus thoraltensis.*

Identification Information	Analysis Time:	4.21 hours	Status:	Final
Selected Organism	91% Probability	*Streptococcus thoraltensis*		
	Bio number:	470410747773231		

Gas chromatography-mass spectroscopic (GC-MS) technique

The result recorded 20 peaks before using the culture filtrate in biosynthesis of Cu NPs (figure 4), and 20 peaks after using the culture filtrate in biosynthesis of Cu NPs (figure 5).

These components that appeared in the *F. oxysporum* culture filtrate were bound to the nanomaterial and disappeared from the remaining *F. oxysporum* culture filtrate after being treated to produce nanoparticles, hexamethyl-Cyclotrisiloxane, Oxime-,methoxy-phenyl-_2-Amino-5-methylbenzoic acid, Benzoic acid, 2-amino-4-methyl-, Dimethoxydimethylgermanium Phthalic acid, isobutyl undec-2-en-1-yl ester, Phthalic acid, 4-cyanophenyl 2-pentyl ester, 1H-Trindene,2,3,4,5,6,7,8,9-octahydro1,1,4,4,9,9-hexamethyl-,3-Hydroxymandelic acid, ethyl ester, di-TMS, Dimethoxydimethylgermanium, Phthalic acid, hept-4-yl tetradecyl ester, Hexatriacontyl pentafluoropropionate, 1-Decanol, 2-hexyl-, Octacosyl trifluoroacetate, 9-Octadecenoic acid, (E)- Cyclohexane,1-(1,5-dimethylhexyl)-4-(4methylpentyl)- Oleic Acid, 1,54-dibromo-1-Hexacosanol, 1,54-dibromo-Octatriacontyl trifluoroacetate, 3,7,11,Trimethyl-8,10- dodecedieny lacetate, 2-Furancarboxylic acid, octadec-9- enyl ester, 1,54-dibromo- , and Hexatriacontyl trifluoroacetate.

Fusarium oxysporum derived antibacterial secondary metabolites most of which are polyketides, followed by Alkaloids, Anthranilates, Aliphatic Acids, Pyran and Furan Derivatives, Phenolic and Aromatic Compounds, *Xanthone* Derivatives, Quinones, Terpenoids, and Cyclopeptides. According to antibacterial properties, Twenty *Fusarium*-derived secondary metabolites were characterized and displayed various bactericidal effects on Gram-positive and Gram-negative strains (21).

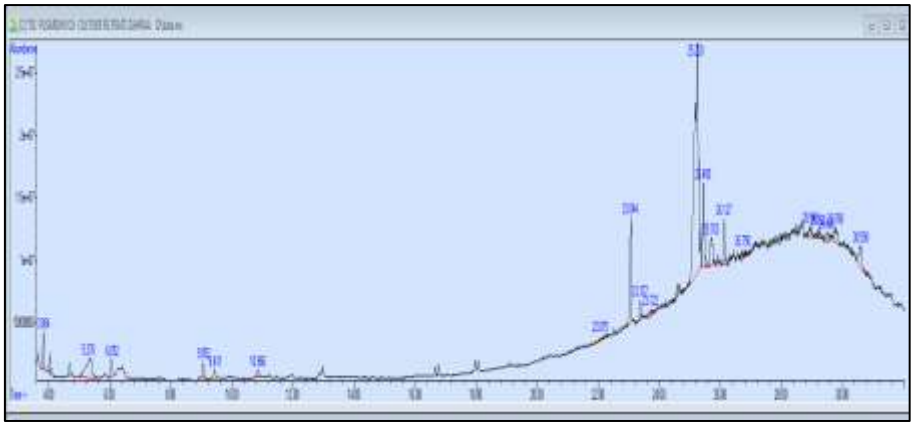

Figure (4): GC-MS analysis of *Fusarium oxysporum* culture filtrate.

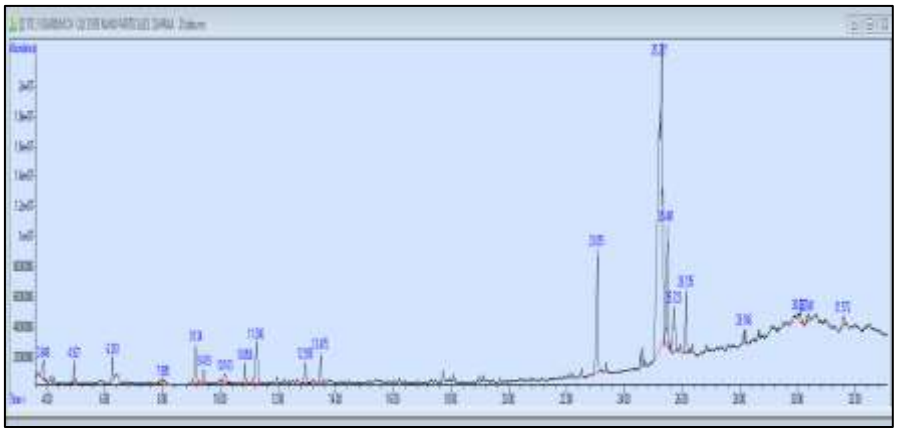

Figure (5): GC-MS analysis of the remaining *Fusarium oxysporum* culture filtrate after being treated to produce nanoparticles.

Biosynthesis of copper nanoparticle (Cu NPs) from *Fusarium oxysporum* culture filtrate

In the current study, *Fusarium oxysporum* culture filtrate was employed to create Cu NPs. Visual monitoring was used to track the reaction mixture's color change. The solution initially changed directly to a green color. The color intensity increased gradually to dark green as the incubation period was lengthened.

Characterization of green synthesis cu nanoparticles

Atomic force microscopy (AFM)

AFM was used to examine the surface appearance of the Cu NPs, the topology of the 2D and 3D Cu NPs was given (Figure 6). The Cu NPs that were created are elongated cuboid-shaped, according to AFM scans, and have an average diameter of 31.33 nm, this result agreed with (22).(Figure 7 and Table 4).

Table (4): The average diameter of Cu nanoparticles synthesized using *F. oxysporum* culture filtrate.

Sample: Cu NPs	Grain No.:8380
Instrument: SPM	Date:2023-01-17
Avg. Diameter: 31.33 nm	<= 10% Diameter: 14.00 nm
<=50% Diameter: 28.00 nm	<=90% Diameter: 52.00 nm

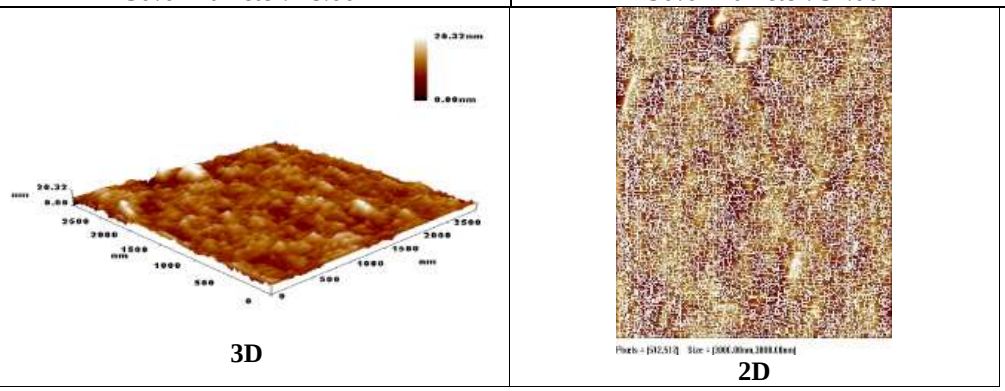

3D **2D**

Figure (6): Atomic force microscopy of Cu NPs 2D and 3D topological

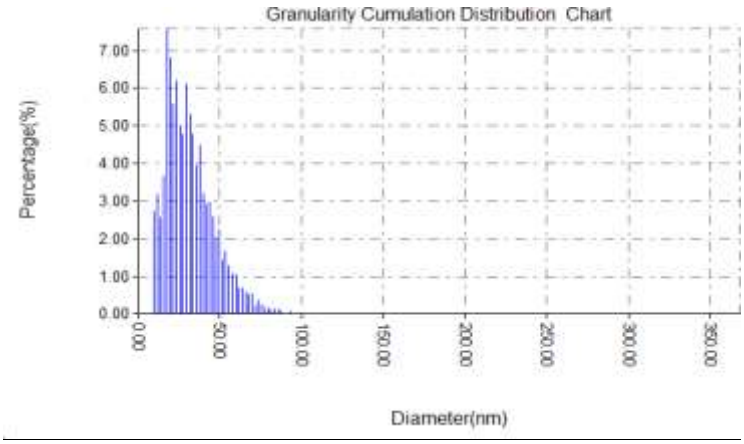

Figure (7): Size of copper nanoparticles on average.

Fourier transform infrared spectroscopy analysis (FTIR)

The spectrum of infrared radiation (IR) was used to measure the outcome at wavelengths between 4000/cm and 500/cm. The FTIR for nano salt powder was 3409.91, 3332.76, 1504.37, 1396.37, 1051.13, 819.69 cm^{-1} (Figure 8). (Figure 9) the FTIR for the combination of salt powder of Copper (II) carbonate basic and *F. oxysporum* culture filtrate may be seen at 3415.70, 1645.17, 1629.74, 1514.02, 1504.37, 1386.72, 1051.13, 819.69, 422.38 cm^{-1}. The result of Cu NPs was 3407.98, 3330.84, 1500.52, 1396.37, 1051.13, 821.62, 580.53, 522.67, 428.17 cm^{-1} (Figure 10). Cu NPs' FTIR spectrum has broad band peaks at 754 cm-1 and 821 cm-1, which is a distinctive peak thought to result from Cu's interaction with culture filtrate's biomolecules, mentioned peaks represent the presence of larger concentrations of alcohols, phenols, alkene, and aldehydes, as well as the O-H and N-H stretches of amino acids. The presence of C=C bending modes of vibration is shown by the absorption peaks exhibited at 1645 cm-1. The final peak at 580 corresponds to the CuO's bending mode s of vibration.

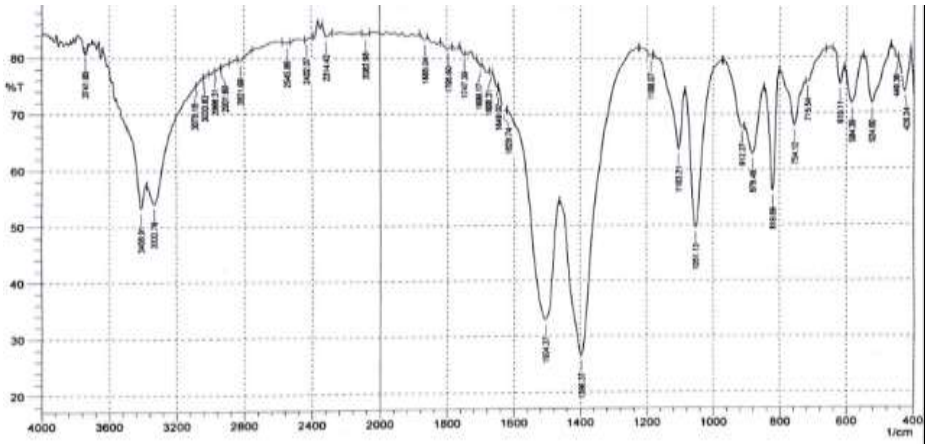

Figure (8): FTIR image of Copper (II) carbonate basic

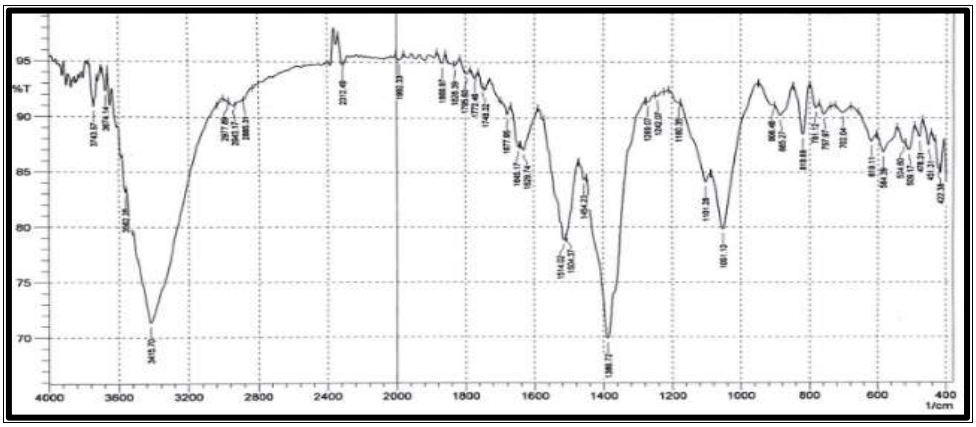

Figure (9): FTIR image of the mixture of *Fusarium oxysporum* culture filtrate and Copper (II) carbonate basic.

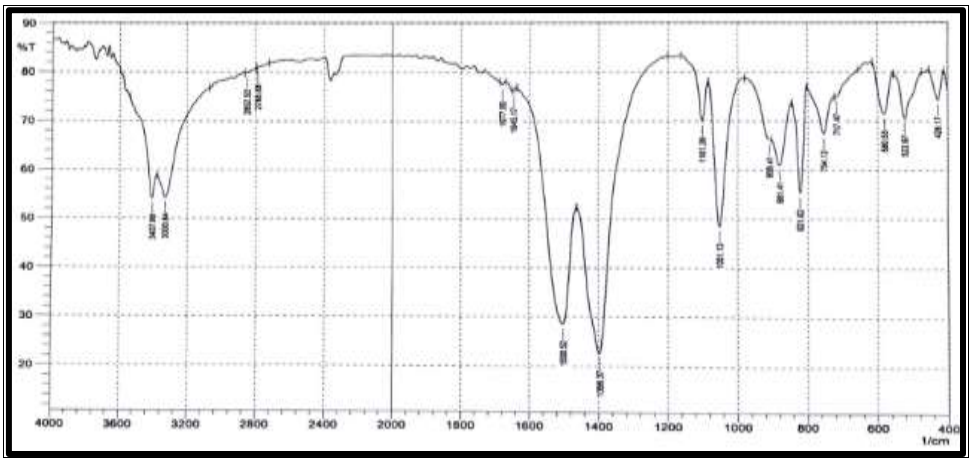

Figure (10): FTIR image of Cu NPs.

Field emission scanning electron microscopy

The FESEM pictures of the copper nanoparticles (Figure 11). Shown the copper nanoparticles surface morphology, look to be elongated cuboids. The particle size histogram in the current study spans the range of 21 to 48 nm. This result strongly confirms that *F. oxysporum* culture filtrate might serve as a reducing and capping agent while creating copper nanoparticles.

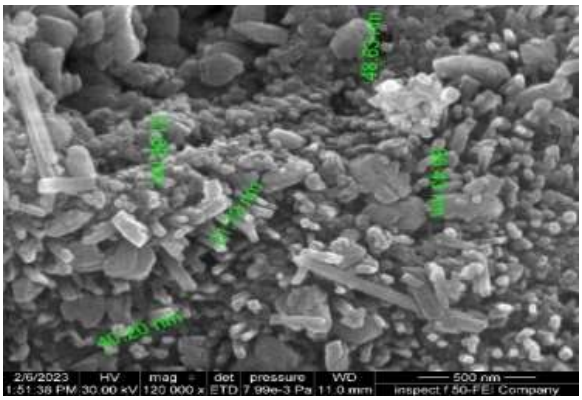

Figure (11): FE-SEM Images of Cu NPs synthesized using *F. oxysporum* culture filtrate.

Energy-dispersive X-ray spectroscopy diffraction technique (EDX)

The EDX spectrum of the synthesized nanoparticles showed in (figure 12), which implies that copper is a component and is present. Surface plasmon resonance is primarily responsible for the typical strong signal peak at 8 keV displayed by metallic copper nanoparticles. Quantitative data of biologically produced Cu NPs and the presence of Cu, O, and C elements shown in the (Figure 13). This finding is consistent with the research findings of (23,24,25).

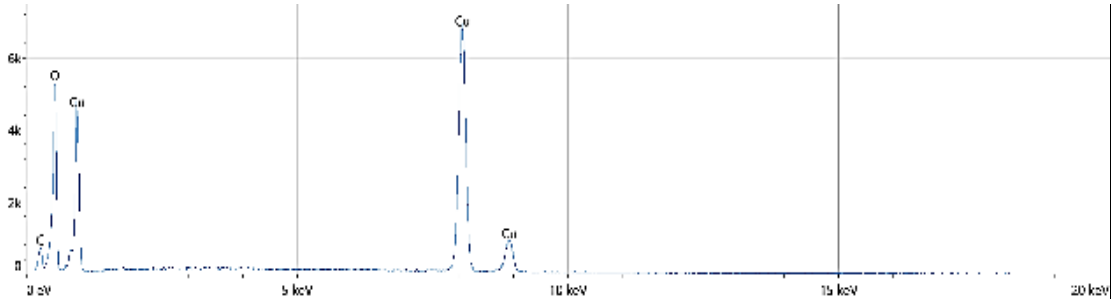

Figure (12): EDX image of prepared Cu nanoparticle.

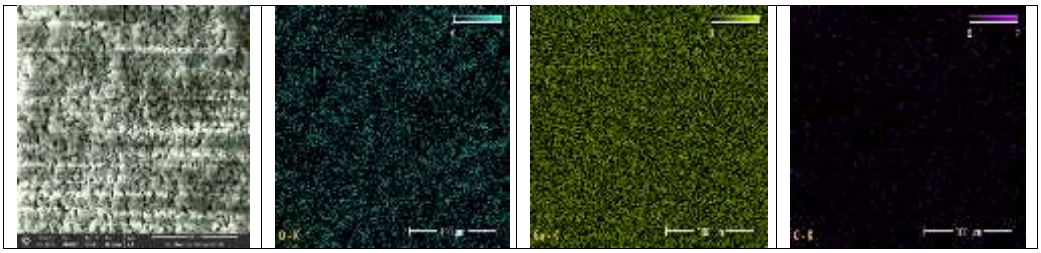

Figure (13): EDX image of Cu nanoparticles elements.

Antibiotics susceptibility

Using the disc diffusion technique advised by the Clinical and Laboratory Standards Institute (CLSI, 2022), the isolates were evaluated for susceptibility to 10 different antibiotics. Depending on the results of the antibiotic susceptibility test Table 5, the tow isolates of bacteria showed multi-drug resistant MDR patterns. *P. mirabilis* isolate was resistant to every antibiotic that was tested, while the *S. thoraltensis* isolate was sensitive only to Azithromycin, Erythromycin, and Levofloxacin. (26 and 27) mentioned the resistance of *S. thoraltensis* to the most antibiotic used in the test. A study done by (28 and 29) agreed with this study showed the resistance of *P. mirabilis* to the most tested antibiotic.

Table (5): The antibiotic susceptibility test results of *Streptococcus thoraltensis* and *Proteus mirabilis* isolates.

Antibiotic	*P. mirabilis*	Antibiotic	*S. thoraltensis*
Piperacillin	R	Meropenem	R
Aztreonam	R	Vancomycin	R
Imipenem	R	Levofloxacin	S
Meropenem	R	Azithromycin	S
Gentamicin	R	Tetracycline	R
Amikacin	R	Tetracycline	R
Ciprofloxacin	R	Chloramphenicol	R
Levofloxacin	R	Ampicillin	R
Ceftazidime	R	Erythromycin	S
Norfloxacin	R	Penicillin	R

Antibacterial susceptibility test

The results of Cu nanoparticles used as antibacterial agents showed antibacterial effects against MDR, results observed significant differences between nanoparticles concentrations, in addition to the presence of significant differences between human pathogenic bacteria Table 6, The findings indicated that the inhibition zone of tested human pathogenic bacteria increased with a rise in NPs concentrations, the maximum inhibition zones of Gram-negative *Proteus mirabilis* were 16 mm at concentration of 500 µg/ml of Cu NPs, whereas the 9 mm minimum inhibition zones when concentration 125 µg/ml of Cu NPs, and Gram-positive *S. thoraltensis* isolate showed significant differences between concentrations, the maximum inhibition zones were 17 mm at concentration of 500 µg/ml of Cu NPs, and the minimum inhibition zones were 9 mm at concentration of 62.5 µg/ml of Cu NPs (figure 14), The results obtained were identical to the search results of (30,31). Because of the significantly varied interactions between Cu NPs and bacteria, there are differences in the diameter of the inhibitory zones. In the current study, Cu NPs produced using *F. oxysporum* culture filtrate had antibacterial properties, when used to treat *S. thoraltensis* bacteria more than for *P. mirabilis*. Perhaps as a result of the high resistance to antibiotics of *P. mirabilis* more than *S. thoraltensis*, and this is probably because of the bacterial cell wall's structure. When compared to Gram-negative bacteria, whose inner wall has an internal barrier made up of a common lipopolysaccharide with multiple proteins that can stop the passage of a lot of lethal substances into the cell, gram-positive bacteria have a greater permeability for materials entering the cell (32). The thickset cell wall may decline the permeation of nanoparticles within cells (33). Researching the superior physicochemical features of NPs and the biological activities of cell membrane vesicles was done by (34). (35) investigated green synthesis of copper nanoparticles as antibacterial. Widespread reports on copper nanoparticles' antibacterial properties relate their ions-released properties to the antimicrobial action. Their small size and high surface-to-volume ratio, which enable them to closely contact with the microbial membranes, further boost the activity. The current study agreed with (36), which found that the CuO NPs formed using the fungi Fusarium oxysporum were extremely stable and effectively combated both Gram-positive and Gram-negative bacteria. As well, Yoon et al explain the antibacterial capabilities of silver and copper nanoparticles using single characteristic strain of *E. coli* When compared to silver nanoparticles, copper nanoparticles showed more antibacterial activity in an experiment with E. coli. (37), and Cuo NPs Synthesized by Staphylococcus epidermidis prepared by (38) showed the antibacterial assay. Additionally, the mechanism of antibacterial activity of Cu NPs studied by (39) who found that Cu NPs treatment resulted in a variety of harmful consequences in *E. coli* cells, including lipid peroxidation, protein oxidation, and DNA damage. Nanoparticles' ability to alternate between cupric and cuprous oxidation states, which produces hydroxyl radicals that bind to DNA molecules and break their helical structure by cross-linking within and between the nucleic acid strands, is what gives them their antimicrobial properties.

Additionally, binding to the carboxyl and sulfhydryl groups of amino acids might harm vital proteins. Similar to how membrane lipids and surface proteins crucial for material transport across cell membranes are eliminated(40).

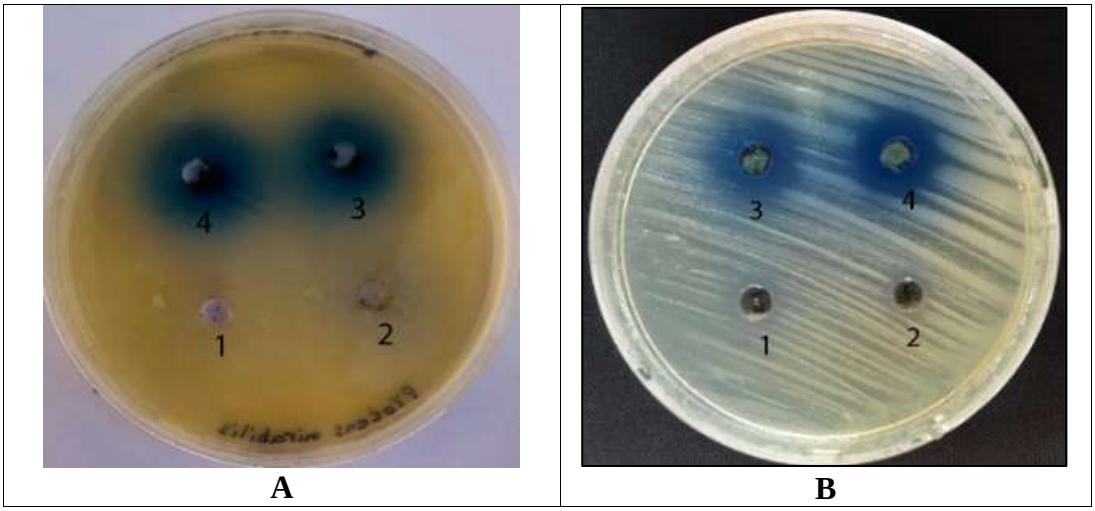

Figure (14): Antimicrobial activity of Cu NPS against (A) *Proteus mirabilis* and (B) *Streptococcus thoraltensis* at different concentrations: (1) 62.5 mg /ml, (2)125 mg /ml, (3) 250 mg /ml, (4) 500 mg /ml.

Table (6): Zone inhibition of human pathogenic bacteria by using Copper nanoparticles of *Fusarium oxysporum* culture filtrate at different concentrations (62.5, 125, 250, and 500mg/ml) on Muller Hinton Agar at pH 7 after 24-48 hours incubated at 37±1˚C.

Bacteria	Zone inhibition (mm)				Average
	NPs 62.5 (mg/ml)	NPs 125 (mg/ml)	NPs 250 (mg/ml)	NPs 500 (mg/ml)	
Proteus mirabilis	0	9.7	11.7	14.7	9
Streptococcus thoraltensis	9.3	10.7	14.3	15.7	12.5
L. S. D	P= 0.05				
Between Bacteria	1.01				
Between concentrations	1.01				
Between interaction	2.04				

*** Each number is an average of three replicate**

Conclusion

The biosynthesis of copper nanoparticles by *Fusarium oxysporum* culture filtrate for the first time as a reducing agent was created successfully, Research findings suggest that copper nanoparticles have higher antibacterial activity on Gram-positive *Streptococcus thoraltensis* bacteria than Gram-negative *Proteus mirabilis* bacteria.

References

1. Ma, L. J.; Geiser, D. M.; Proctor, R. H.; Rooney, A. P.; O'Donnell, K.; Trail, F., *et al*. (2013). Fusarium pathogenomics. Annual Review of Microbiology, 67, 399 - 416.
2. Fu, Y.; Wu, P.; Xue, J.; Zhang, M. and Wei, X. (2020). Cosmosporasides F-H, three new sugar alcohol conjugated acyclic sesquiterpenes from a Fusarium oxysporum fungus. Natural Product Research, 1–9.
3. Korbekandi, H.; Ashari, Z.; Iravani, S. and Abbasi, S. (2013). Optimization of Biological Synthesis of Silver Nanoparticles using *Fusarium oxysporum*. Iranian journal of pharmaceutical research: IJPR, 12(3): 289.

4. Elazab, N. T.; Younis, S. A. and Abdelgalil, S. A. (2023). Biogenic Synthesis of Nanoparticles Mediated by Fungi. Plant Mycobiome: Diversity, Interactions and Uses, 241-265.
5. Kimber R. L.; Lewis E. A.; Parmeggiani F.; Smith K.; Bagshaw H. Starborg T., *et al*. (2018). Biosynthesis and characterization of copper nanoparticles using Shewanella oneidensis application for click chemistry. Small, 14(10): 1703145.
6. Gawande M.; Goswami A.; Felpin F.; Asefa T.; Huang X.; Silva R., *et al*. (2016). Cu and Cu-based nanoparticles: synthesis and applications in catalysis. Chemical Reviews, 116(6): 3722-3811.
7. Zaboon, S. and Al-Hayanni, H. (2021). Detection of virulence factor genes and antibiotic resistance of Enteropathogenic *Escherichia coli* (EPEC) isolated from children with diarrhea. Biochemical and Cellular Archives, 21(1): 791-796.
8. Sedláková, M.; Urbánek, K.; Vojtová, V.; Suchánková, H.; Imwensi, P. and Kolář, M. (2014). Antibiotic consumption and its influence on the resistance in Enterobacteriaceae. BMC Research Notes 7: 1-10.
9. Lekshmi, M.; Ammini, P.; Kumar S. and Varela M. (2017). The food production environment and the development of antimicrobial resistance in human pathogens of animal origin. Microorganisms, 5: 11–25.
10. Sohn, K.M.; Kang, C.I.; Joo, E.J.; Ha, Y.E.; Chung, D.R.; Peck, K.R.; Lee, N.Y.; Song, J.H. (2011). Epidemiology of ciprofloxacin resistance and its relationship to extended-spectrum βlactamase production in *Proteus mirabilis* bacteremia. The Korean Journal of Internal Medicine, 26(1): 89-93.
11. Jacobsen, S. M.; Lane, M. C.; Harro, J. M.; Shirtliff, M. E. and Mobley, H. L. (2008). The high-affinity phosphate transporter Pst is a virulence factor for *Proteus mirabilis* during complicated urinary tract infection. FEMS Immunology and Medical Microbiology, 52(2): 180-193.
12. Moreno, L.Z.; Matajira, C.E.C.; Gomes, V.T.M.; Silva, A.P.S.; Mesquita, R.E.; Christ, A.P.G., *et al*. (2016). Molecular and antimicrobial susceptibility profiling of atypical *Streptococcus* species from porcine clinical specimens. Infection, Genetics and Evolution, 44: 376-381.
13. Abbas, H. and Hegazy, W. (2020). Repurposing anti-diabetic drug "Sitagliptin" as a novel virulence attenuating agent in Serratia marcescens. PLoS One, 15(4): e0231625.
14. Nelson, P.; Toussoun, T. and Marasas, W. (1983). *Fusarium* Species: An Illustrated Manual for Identification. Pennsylvania State University Press, University Park, Pennsylvania, USA.
15. Watanabe, T. (2002). Pictorial atlas of soil and seed fungi: morphologies of cultured fungi and key to species. 2nd ed. CRC press. Washington, D.C.
16. Yaaqoob, L. (2022). Evaluation of the Biological Effect Synthesized Iron Oxide Nanoparticles on Enterococcus Faecalis, Iraqi Journal of Agricultural Sciences, 53: 440.
17. Al-Adhami, N. and Al-Araji, A. (2019). Molecular characterization by PCR-ITS technique of *Fusarium oxysporum* isolated from tomato in Baghdad city. Tikrit Journal of Pure Science, 24(3): 31-43.
18. Hasan, A. M., Naji, E. N., and Khelkal, I. N. (2022). molecular characterization of adhesion genes in some oral bacteria. Biochemical and Cellular Archives, 22(1).
19. Agha, Z. H. M., and Al-Delaimi, M. S. (2021). Prevalence of common bacterial etiology and antimicrobial susceptibility pattern in patients with otitis media in Duhok Province–Iraq. Zanco Journal of Pure and Applied Sciences, 33(4), 11-25.
20. Ghafil, J. A., and Flieh, M. (2021). Isolation and Identification of Bacterial Burn Wound Infection in Iraqi Patient. Indian Journal of Forensic Medicine and Toxicology, 15(4).
21. Xu, X., Shen, G., Teng, H., Zhao, J., Xiao, J., Guo, L., ... and Zhao, J. (2023). Unravelling Species Diversity and Pathogenicity of *Fusarium spp*. associated with soybean leaf and root in Heilongjiang Province, China. Plant Disease, (ja).
22. Rajeshkumar, S., et al. (2022). "Evaluation of zebrafish toxicology and biomedical potential of aeromonas hydrophila mediated copper sulfide nanoparticles." Oxidative Medicine and Cellular Longevity 2022.
23. Kaviya, S., et al. (2011). "Biosynthesis of silver nanoparticles using Citrus sinensis peel extract and its antibacterial activity." Spectrochimica Acta Part A:

Molecular and Biomolecular Spectroscopy 79.3: 594-598.
24. Magudapathy, P., et al. (2001). "Electrical transport studies of Ag nanoclusters embedded in glass matrix." Physica B: Condensed Matter 299.1-2: 142-146.
25. Das, J., M. Paul Das, and P. Velusamy (2013). "Sesbania grandiflora leaf extract mediated green synthesis of antibacterial silver nanoparticles against selected human pathogens." Spectrochimica Acta Part A: Molecular and Biomolecular Spectroscopy 104: 265-270.
26. Torres, M. C., Moni, C. A., Menetrier, L. D. C., Breyer, G. M., and Siqueira, F. M. (2022). *Streptococcus spp*. in equines: infection and antimicrobial susceptibility profiles. Acta scientiae veterinariae. Porto Alegre, RS. Vol. 50, Pub. 1882, 5 p.
27. Al-Tamimi, M., Himsawi, N., Abu-Raideh, J., Abu Jazar, D., and Al-Jawaldeh, H. (2019). Isolation of fully vancomycin-resistant *Streptococcus thoraltensis* from the nasal cavity of a healthy young adult. Microbial Drug Resistance, 25(3), 421-426.
28. Al-Bassam, W. W., and Al-Kazaz, A. K. (2013). The isolation and characterization of *Proteus mirabilis* from different clinical samples. Journal of Biotechnology Research Center, 7(2), 24-30.
29. Alhusayni, A. A., Al-Khikani, F. H. O., Aljaburi, H. K., Alkareawiu, B. A. A., and Abadi, R. M. (2022). Antibiotic susceptibility profile of bacterial uropathogens in Al-Shomali General Hospital, Babylon, Iraq. Journal of Preventive, Diagnostic and Treatment Strategies in Medicine, 1(4), 240.
30. Alnuaimi, M.; AL-Hayanni, H. and Aljanabi, Z. (2023). Green synthesis of gold nanoparticles from Sophora flavescens extract and their antibacterial effect against some pathogenic bacteria. Malaysian Journal of Microbiology, 19(1): 74-82.
31. Yaaqoob, A. and Qasem, M. (2022). Effectivity of Iron Oxide Nanoparticles Synthesis by Intracellular Lactobacillus as Antibacterial Agent against *Pseudomonas aeruginosa*. Iraqi Journal of Biotechnology, 21(2).
32. Al-Mossawei, M.; Ali, A.; Abid, H. and Murad, R. (2014). Antimicrobial activity of ethanolic extracts of *Raphanus sativus* and *Cyperus rotundus* against some pathogenic bacteria and *Candida albicans*. Baghdad Science Journal, 11(2): 748-756.
33. Abdulhadi, S. M., Shami, A. M., & Saleh, M. M. (2020). Antibacterial effect, Antioxidant potential and total phenolic content of polyphenol extracts of *Myrtus communis* leaves. Plant Archives, 20(2), 286-291.
34. Ma, J.; Jiang, L. and Liu, G. (2022). Cell membrane coated nanoparticles for the treatment of bacterial infection. Wiley Interdisciplinary Reviews: Nanomedicine and Nanobiotechnology, 14(5): e1825.
35. Al-Jubouri, A.; Al-Saadi, N. and Kadhim, M. (2022). Green synthesis of copper nanoparticles from *Myrtus communis* leaves extract: characterization, antioxidant, and catalytic activity. Iraqi Journal of Agricultural Sciences, 53(2): 471-486.
36. Majumder, B. (2012). Bioremediation: Copper Nanoparticles from Electronic-waste, International Journal of Engineering Science and Technology, 4(10).
37. Yoon, J.; Byeon, J.; Park, J. and Hwang, (2007). Susceptibility constants of *Escherichia coli* and *Bacillus subtilis* to silver and copper nanoparticles, Sci Total Environ, 373: 572–575.
38. Zahraa, H.; Kadhim, Mais, E. and Ahmed, I. Ş. (2023). Antibacterial and Cytotoxic Effect of Synthesized Cuo NPs from *Staphylococcus epidermidis* Iraqi Journal of Biotechnology. 22(1): 173-182.
39. Chatterjee, A.; Chakraborty, R. and Basu T. (2014). Mechanism of antibacterial activity of copper nanoparticles. Nanotechnology, 25: 135101.
40. Aslam, M.; Gopakumar, G.; Shoba, T.; Mulla, I.; Vijayamohanan, K.; Kulkarni, S., *et al*. (2002). Formation of Cu and Cu2O nanoparticles by variation of the surface ligand: preparation, structure, and insulating-to-metallic transition. Journal of Colloid and Interface Science, 255(1): 79-90.